Kinetics of Ozone Photolysis in Aqueous Solution

Mirat D. Gurol and Aysegul Akata
Dept. of Chemical Engineering and Environmental Studies Institute, Drexel University, Philadelphia, PA 19104

The kinetics of ozone photolysis were investigated experimentally in well-characterized aqueous solution and by a conceptual kinetic and mechanistic model developed based on possible reaction pathways. The primary quantum yield of ozone photolysis at 254-nm wavelength was measured at 20°C as 0.48 ± 0.6. The rate of ozone photolysis increased with increasing light intensity, ozone concentration and pH, and decreased with increasing inorganic carbon concentration in water. The model was able to predict the experimentally observed rate of ozone photolysis quite well for various combinations of UV light intensity, initial ozone concentration and water characteristics. In the mechanistic model, the formation of the hydroxyl radical, which is the primary oxidant in the O_3/UV process, was tied to the decomposition of ozone; therefore, the model can now be extended to predict the oxidation rates of water contaminants by the hydroxyl radical generated in the O_3/UV process.

Introduction

The process of ozonation coupled with ultraviolet radiation (O_3/UV) is one of the most effective chemical oxidation techniques for treatment of contaminated waters and wastewaters. This process is capable of oxidizing organic substances at ambient temperature and pressure to innocuous reaction products, such as carbon dioxide, carboxylic acids, and halide ions. Since the mid-1970s, it has been applied for oxidation of cyanides in wastewaters (Garrison et al., 1975) as well as synthetic organic compounds, for example, oxalic and acetic acids (Kuo et al., 1977), methyl and ethyl alcohol (Ikemizu et al., 1987), and trichloroethane, trichloroethylene, tetrachloroethylene, and chloroform in surface and groundwater (U.S. EPA Report, 1990). Pentachlorophenol and other substituted phenols were oxidized successfully treated by application of the same process (Gurol and Vatistas, 1987; Johnson and Gurol, 1988). The O_3/UV process was also used to eliminate the natural organic matter in water in order to reduce the subsequent formation of trihalomethanes (Glaze et al., 1983; Arai et al., 1992; Akata and Gurol, 1992).

The process of oxidation by the O_3/UV process in a reactor requires an understanding of the mechanism of ozone photolysis under UV exposure, the chemical oxidation of the organic compounds, and kinetics of ozone transfer from gas phase into aqueous solution. However, very few of the studies reported in the literature have addressed these fundamental aspects of the process, or made an attempt to differentiate among the physical and chemical reaction steps. Generally, the studies were confined to the process feasibility under limited conditions (Kearney et al., 1987); otherwise, the process was described by empirical models (Khan et al., 1985; Prengle, 1983; Barker and Taylor, 1985; Peyton et al., 1982). These models, which use system-specific lumped parameters, are inadequate to describe the process under different operational conditions.

The first attempt to identify the mechanism of ozone photolysis was made by Peyton and Glaze (1988), who confirmed the formation of hydrogen peroxide as the first reaction intermediate of ozone photolysis. It was also proposed that the secondary reactions lead to the production of hydroxyl radical ($OH^{\cdot}$), the major oxidant in the O_3/UV process. However, very few detailed investigations have been made regarding the kinetics and mechanism of the radical chain reactions that describe the initial and the subsequent reactions of ozone photolysis. Ikemizu et al. (1987) reported a decomposition rate for ozone that was first order with respect to both ozone concentration and UV light intensity, in the range of 0.03–0.4 mol/m^3 of ozone and 2–40 $W \cdot m^{-2}$ of light intensity. The decomposition rate showed slight dependence on pH of solution in the pH range of 2–9. Based on this empirical-rate expression, the overall quantum yield of ozone decomposition in aqueous solution without radical scavengers was estimated to be greater than 3 (Morooka et al., 1988). Yao et al. (1992) attempted to model the oxidation of butyric acid based

Correspondence concerning this article should be addressed to M. D. Gurol.

on an extensive list of reactions by assigning values for several unknown constants at pH 2 and 7.

Hence, additional research is needed in order to quantify the rate of ozone photolysis and oxidation of organic compounds by hydroxyl radical and by direct photolysis. To be able to characterize the process effectively under various operating and water-quality conditions, these reactions should be investigated separately, and incorporated into a comprehensive process model that also includes an expression for the rate of mass transfer of ozone (Akata, 1994). The objective of the present article is to investigate the kinetics of ozone photolysis experimentally in a batch system under controlled conditions based on the kinetic model composed of anticipated elementary reaction steps. In this study, ozone was dissolved in water before being exposed to UV light in order to eliminate the mass-transfer considerations for ozone. The effects of light intensity, ozone concentration, and the water characteristics were studied systematically. The experimental results were then compared to the model predictions for confirmation and verification of the kinetic model.

Mechanism of Ozone Photolysis

The principal reactions anticipated during ozone photolysis in pure water, as presented by Peyton and Glaze (1988), are listed below:

Initiation/Light Absorption

$$O_3 + H_2O \xrightarrow{h\nu} H_2O_2 + O_2 \qquad \phi_p I_a \qquad (1)$$

Propagation

$$H_2O_2 \xrightarrow{h\nu} 2OH^{\cdot} \qquad \phi'_p I'_a \qquad (2)$$

$$H_2O_2 \Leftrightarrow HO_2^- + H^+ \qquad pK_{a,3} \qquad (3)$$

$$HO_2^- + O_3 \rightarrow O_3^{\cdot -} + HO_2^{\cdot} \qquad k_4 \qquad (4)$$

$$HO_2^{\cdot} \Leftrightarrow H^+ + O_2^{\cdot -} \qquad pK_{a,5} \qquad (5)$$

$$O_2^{\cdot -} + O_3 \rightarrow O_3^{\cdot -} + O_2 \qquad k_6 \qquad (6)$$

$$O_3^{\cdot -} + H^+ \rightarrow OH^{\cdot} + O_2 \qquad k_7 \qquad (7)$$

$$OH^{\cdot} + H_2O_2 \rightarrow HO_2^{\cdot} + H_2O \qquad k_8 \qquad (8)$$

$$OH^{\cdot} + HO_2^- \rightarrow HO_2^{\cdot} + OH^- \qquad k_9 \qquad (9)$$

$$OH^{\cdot} + O_3 \rightarrow HO_2^{\cdot} + O_2 \qquad k_{10} \qquad (10)$$

Termination

$$2OH^{\cdot} \rightarrow H_2O_2 \qquad k_{11} \qquad (11)$$

$$2HO_2^{\cdot} \rightarrow H_2O_2 + O_2 \qquad k_{12} \qquad (12)$$

$$HO_2^{\cdot} + O_2^{\cdot -} + H_2O \rightarrow H_2O_2 + O_2 + OH^- \qquad k_{13} \qquad (13)$$

According to this reaction scheme, photolysis of aqueous ozone produces hydrogen peroxide as the primary product (Reaction 1), which then can photolyze directly into hydroxyl radical (Reaction 2). In addition, the dissociated form of hydrogen peroxide, peroxy ion (HO_2^-), reacts also with ozone (Reaction 4). This reaction leads to the production of ozonide ion ($O_3^{\cdot -}$) and hydroperoxide radical ($HO_2^{\cdot}$), both of which produce hydroxyl radical as shown by Reactions 5 to 7. Hydrogen peroxide and ozone consume hydroxyl radical, as indicated in Reactions 8 to 10. However, these reactions also propagate by producing the superoxide radical ($HO_2^{\cdot -}$), which reacts with ozone to generate more hydroxyl radical. In pure water, chain reactions can be terminated by radical–radical reactions between the chain carriers $OH^{\cdot}$, $O_2^{\cdot -}$, $HO_2^{\cdot}$, as described by Reactions 11–13.

In pure water decomposition of ozone is also initiated by hydroxide ion (Staehelin and Hoigne, 1982):

$$O_3 + OH^- \rightarrow HO_2^{\cdot} + O_2^{\cdot -} \qquad k_{14}. \qquad (14)$$

Although this reaction was included in the overall reaction scheme, it has to be noted that ozone decomposition by this reaction is too slow compared to ozone decomposition under UV exposure.

In natural water, bicarbonate and carbonate ions, which are generally abundant, can participate in various reactions with the free radicals. These ions might serve as the major inorganic scavengers of hydroxyl radical (Staehelin and Hoigne, 1982) as well as the chain carries (Peyton and Glaze, 1988; Liao and Gurol, 1995) as shown below:

$$OH^{\cdot} + HCO_3^- \rightarrow HCO_3^{\cdot} + OH^- \qquad k_{15} \qquad (15)$$

$$OH^{\cdot} + CO_3^{=} \rightarrow CO_3^{\cdot -} + OH^- \qquad k_{16} \qquad (16)$$

$$HCO_3^- \Leftrightarrow H^+ + CO_3^{=} \qquad pK_{a,17} \qquad (17)$$

$$HCO_3^{\cdot} \Leftrightarrow H^+ + CO_3^{\cdot -} \qquad pK_{a,18} \qquad (18)$$

$$CO_3^{\cdot -} + H_2O_2 \rightarrow HO_2^{\cdot} + HCO_3^- \qquad k_{19} \qquad (19)$$

$$CO_3^{\cdot -} + HO_2^- \rightarrow O_2^{\cdot -} + HCO_3^- \qquad k_{20} \qquad (20)$$

$$HCO_3^{\cdot}/CO_3^{\cdot -} + I \rightarrow \text{Products} \qquad k_i \qquad (21)$$

Here the reactions of hydroxyl radical with bicarbonate and carbonate ions (Reactions 15 and 16) produce bicarbonate and carbonate radicals ($HCO_3^{\cdot}$ and $CO_3^{\cdot -}$), which propagate the chain by reacting with hydrogen peroxide (Reactions 19 and 20). These radicals might also react with other scavengers (I) present in water matrix, as shown by Reaction 21. The rate and equilibrium constants for Reactions 3–20 reported for room temperature (20–23°C) are presented in Table 1.

Kinetic Model

According to the reaction mechanism proposed for pure water, decomposition of ozone is initiated by its interaction with UV light, which constitutes the primary step of photolysis, and the subsequent radical reactions further contribute to decomposition of ozone. Hydrogen peroxide is expected to be the only stable reaction intermediate. Based on this proposed mechanism, the overall rate of change in the concentrations of dissolved ozone and hydrogen peroxide in a batch reactor can be expressed as follows:

$$-d[O_3]/dt = \phi_p I_a + k_4[HO_2^-][O_3] + k_6[O_2^{\cdot -}][O_3] + k_{10}[OH^{\cdot}][O_3] + k_{14}[OH^-][O_3] \qquad (22)$$

$$d[H_2O_2]/dt = \phi_p I_a + k_{11}[OH^{\cdot}]^2 + k_{12}[HO_2^{\cdot}]^2 + k_{13}[HO_2^{\cdot}][O_2^{\cdot -}] - \phi'_p I'_a - k_4[HO_2^-][O_3] - k_8[OH^{\cdot}][H_2O_2] - k_9[OH^{\cdot}][HO_2^-] - k^*_{19}[H_2O_2][CO_3^{\cdot -}] \qquad (23)$$

Table 1. Rate and Equilibrium Constants for Principal Reactions of Ozone Photolysis

Constant	Rate Constant ($M^{-1}\cdot s^{-1}$) Equilibrium Constant (pK_a)	Reference
$pK_{a,3}$	11.8	Sauer et al., 1984
k_4	2.8×10^6	Staehelin and Hoigne, 1982
$pK_{a,5}$	4.8	Rabani and Nielsen, 1969
k_6	1.6×10^9	Buhler et al., 1984
k_7	5.2×10^{10}	Buhler et al., 1984
k_8	2.7×10^7	Christensen et al., 1982
k_9	7.5×10^9	Christensen et al., 1982
k_{10}	3.0×10^9	Bahnemann and Hart, 1984
k_{11}	5.5×10^9	Farhataziz and Ross, 1977
k_{12}	7.6×10^5	Bielski and Allen, 1977
k_{13}	8.9×10^7	Bielski and Allen, 1977
k_{14}	70	Staehelin and Hoigne, 1982
k_{15}	3.6×10^7	Weeks and Rabani, 1966
k_{16}	4.2×10^8	Weeks and Rabani, 1966
$pK_{a,17}$	10.3	Larson and Buswell, 1942
$pK_{a,18}$	7.9	Eriksen et al., 1985
k_{19}	8.0×10^5	Behar et al., 1970
k_{20}	5.6×10^7	Behar et al., 1970

where

$$k_{19}^* = (k_{19}[H^+] + k_{20}K_{a,3})/[H^+] \quad (24)$$

The term $\phi_p I_a$ represents the decomposition rate of ozone by the initiation reaction. The ϕ_p is the primary quantum yield of ozone photolysis, which is defined as the number of moles of ozone decomposed per mole of light photons absorbed by ozone. The I_a is the average rate of photon absorption by dissolved ozone. The *average* primary decomposition rate of ozone can be expressed explicitly on the basis of the Beer's Law as follows:

$$-(d[O_3]/dt)_p = \phi_p I_a = \phi_p I_o(1 - e^{-2.3A}) \quad (25)$$

where I_o is the incident UV light intensity and A is the average light absorption by ozone. The absorption coefficient for ozone has been reported to be 3,600 $M^{-1}\cdot cm^{-1}$ at a wavelength of 254 nm (Bahneman and Hart, 1984). Due to the strong light absorption, I_a can be assumed to be about equal to I_o, that is, ozone functions like an actinometer. As a result, Eq. 25 can be simplified into Eq. 26:

$$-(d[O_3]/dt)_p = \phi_p I_o \quad (26)$$

The term, $\phi'_p I'_a$ in Eq. 23 describes the *average* decomposition rate of H_2O_2 by the primary photolysis step. The ϕ'_p is the primary quantum yield and I'_a is the rate of UV light absorption by H_2O_2. It should be noted that H_2O_2 does not absorb UV light strongly, and a', which is the absorption coefficient for H_2O_2, is only 19.6 $M^{-1}\cdot cm^{-1}$ at 254 nm (Baxendale and Wilson, 1956). As a result, Eq. 27, which describes the rate of primary photolysis of hydrogen peroxide in planar geometry according to the Beer Lambert Law, can be reduced to Eq. 28 for low concentrations of hydrogen peroxide based on Taylor series expansion:

$$(d[H_2O_2]/dt)_p = \phi'_p I'_a = \phi'_p I_o(1 - e^{-2.3a'b'[H_2O_2]}) \quad (27)$$

$$= 2.3\phi'_p a' b' I_o [H_2O_2] \quad (28)$$

The path length of the light at a given wavelength (b) depends upon the type, the geometry, and the construction material of a reactor as well as the transmitting medium and the type of the absorbing molecule. Since the reactor used in this study has a cylindrical geometry, and the primary interest in this study is to determine the spatial-*average* rates of reactions involving average concentrations of ozone and hydrogen peroxide rather than the exact distribution of light intensity within the reactor, the average hydrogen peroxide rate of change in our reactor can be described by the following semiempirical expression:

$$(d[H_2O_2]/dt)_p = 2.3\phi'_p a' b_{eff} I_o [H_2O_2] \quad (29)$$

where b_{eff} is called the "effective" optical pathlength of UV light in the experimental reactor for hydrogen peroxide.

To be able to evaluate the experimental results based on the kinetic expressions given by Eqs. 22–29, the primary quantum yield for ozone photolysis (ϕ_p) and the "effective" optical pathlength of UV light in the experimental reactor for hydrogen peroxide need to be determined independently. The primary quantum yield for hydrogen peroxide photolysis (ϕ'_p) is already provided in the literature as 0.5 (Hunt and Taube, 1952; Baxendale and Wilson, 1956).

Experimental Methods

The apparatus used in this study includes an ozone gas generator, a photochemical chamber, a reaction vessel, and two UV spectrophotometers for ozone measurements (Figure 1). The experiments were conducted under batch conditions in a quartz vessel. The vessel was placed in a chamber that contained concentrically placed 16 removable low-pressure mercury lamps that emit UV light primarily at 254 nm (that is, 93% of the light emitted in the UV range) at a power rated as 2.2 W per lamp. The UV dosage was controlled by keeping the desired number of UV lamps in the chamber. The cylindrical reaction vessel had an inner diameter of 13 cm, and was filled to contain 2 L of solution during experiments. It was equipped with openings for ozone gas inlet and

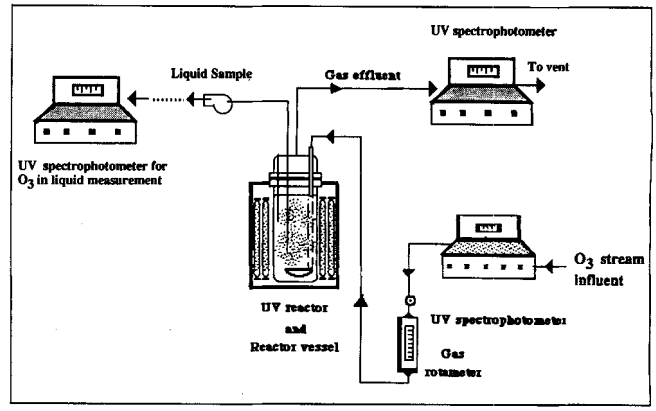

Figure 1. Experimental setup.

outlet for liquid sampling. A glass diffuser was used to sparge ozone gas into the solution. The solution in the reaction vessel was mixed by a magnetic stirrer during ozonation and the UV exposure, and the experiments were conducted at a temperature of 20 ± 1°C. The increase in the temperature of the solutions due UV exposure was less than 1°C. Ozone gas was generated from oxygen by using Welsbach T-408 ozone generator. Ozone gas concentration in the influent and effluent gas was measured continuously by a UV spectrophotometer that was calibrated by the potassium iodide method (*Standard Methods*, 1985).

Ozone/oxygen gas was bubbled into the reaction vessel containing the solution for about 10 minutes until steady-state conditions were reached. The gas flow was then turned off. The initial dissolved ozone concentration in solution was measured as 0.08–0.25 mM, depending on the pH of the solution. The solution was then exposed to the UV radiation at an incident light intensity of 1.5×10^{-6} to 5.8×10^{-6} einstein/L-s. The decomposition of ozone as a function of time was measured by pumping the reactor content continuously through a flow cell placed in a UV spectrophotometer. The dissolved ozone concentration was monitored by measuring the UV absorbance of the solution at a wavelength of 258 nm. The spectrophotometers were calibrated by the potassium iodide method (*Standard Methods*, 1985). The range of reproducibility with this technique was $\pm 5\%$ of the average ozone concentration.

The intensity of the UV lamps as received in the reactor was measured by the method of ferrioxalate actinometry (Parker, 1953; Hatchard and Parker, 1956). In this method, ferrioxalate is reduced by UV light to ferrous iron, which forms a stable complex with 1,10-phenanthroline. The ferrous-1,10-phenanthroline complex can be detected by a spectrophotometer at a wavelength of 551 nm. The ferrioxalate solution was radiated under exactly the same conditions as ozone photolysis, and the light intensity received was estimated based on a quantum yield of 1.25 mole ferrous iron formed per einstein light photons absorbed by the actinometer (Parker, 1953; Hatchard and Parker, 1956). The number of UV lamps used in the photochemical chamber vs. the UV light intensity measured by actinometry is presented in Figure 2.

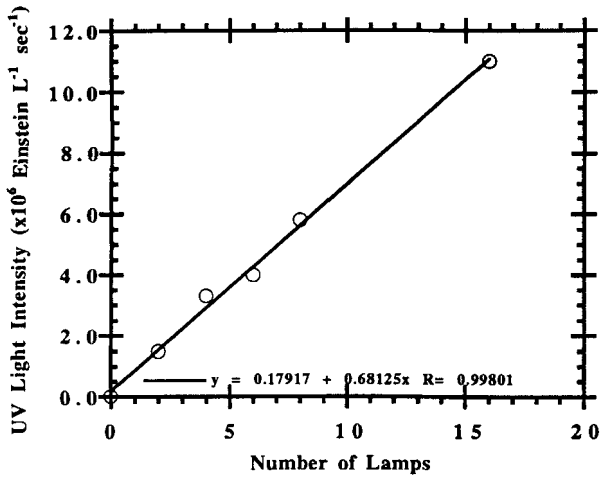

Figure 2. UV light intensities vs. number of UV lamps.

The concentration of hydrogen peroxide in solution was determined by the method of horseradish peroxidase–catalyzed oxidation of *N,N*,diethyl-*p*-phenylene-diamine (DPD) (Bader and Hoigne, 1988). Samples of 10 mL were taken from the reaction vessel and transferred into the vials containing horseradish peroxidase and DPD. The color of solutions was quantified as light absorbance at 558 nm. Hydrogen peroxide (% 30) was purchased from Fisher Chemical company. Horseradish peroxidase and *N,N*-diethyl-*p*-phenylene-diamine were obtained from Sigma Chemical. Potassium trioxalatoferrate was purchased from Alfa company.

The aqueous solution was prepared with or without ACS-certified sodium bicarbonate to adjust the total inorganic carbon concentrations (C_T) in the range of 0–10 mM. The pH was then adjusted to 2–9 by dilute H_2SO_4 and NaOH solutions. For measurement of the primary quantum yield for ozone photolysis, additional experiments were conducted on concentrated HCl solutions (0.02–0.2 N). The optical path length of the experimental system was measured by using solutions of hydrogen peroxide (0.23 mM) in the presence of allyl alcohol ($CH_2 = CH - CH_2OH$), as described later in the text.

Primary Quantum Yield of Ozone Photolysis

According to the presented mechanism of ozone photolysis, the primary decomposition rate of ozone is expected to be equivalent to the overall decomposition rate in a medium where the secondary chain reactions of ozone with HO_2^-, $O_2^{\cdot -}$, and $OH^{\cdot}$, and the decomposition of ozone initiated by OH^- are inhibited. The reactions of ozone with HO_2^- and $O_2^{\cdot -}$ and OH^- can be eliminated in a highly acidic solution where these species exist in negligible concentrations (pK_a of H_2O_2, $HO_2^{\cdot}$ and H_2O are 11.8, 4.8, and 14, respectively). Furthermore, in the presence of a high concentration of an $OH^{\cdot}$ scavenger, the reaction of $OH^{\cdot}$ with ozone is expected to be eliminated as well. Thus, the average overall ozone decomposition rate under these conditions can be expressed as a zero-order reaction, as presented by Eq. 26. Integration of Eq. 26 results in

$$[O_3] = [O_3]_o - \phi_p I_o t = [O_3]_o - k_o t \qquad (30)$$

where $[O_3]_o$ is the initial ozone concentration and $[O_3]$ is the average ozone concentration at time t in solution. Hence, when the experimental data are obtained in the acidic solution containing radical scavengers, ozone concentration as a function of time is expected to produce a straight line. The ϕ_p can then be determined by plotting the slope (k_o) obtained at various light intensities (I_o) as a function of the corresponding light intensity.

Concentrated HCl solutions were used for determination of the primary quantum yield. Since the Cl^- ion is highly reactive toward $OH^{\cdot}$ radical, concentrated HCl solution is expected to work as an effective trap for $OH^{\cdot}$ radicals. The reaction of Cl^- with the $OH^{\cdot}$ radical might lead to a set of chain reactions that are presented in Table 2 (Jayson et al., 1972; Chameides and Stelson, 1992). The initial reaction of $OH^{\cdot}$ with Cl^- produces $Cl^{\cdot}$ which further reacts with Cl^- to produce $Cl_2(g)$. These reactions can also produce $HO_2^{\cdot}$; however, since no appreciable amounts of $O_2^{\cdot -}$ will be present in

Table 2. The Anticipated Reactions of Cl^- in O_3/UV Process

Reaction	Equilibrium or Rate Constant
$OH^{\cdot}+Cl^-+H^+ \rightarrow H_2O+Cl^{\cdot}$	$2.0\times10^{10}\ M^{-2}\cdot s^{-1}$
$Cl^{\cdot}+Cl^- \Leftrightarrow Cl_2^-$	$2\times10^5\ M$
$Cl_2^- + Cl_2^- \rightarrow Cl_2(g)+2Cl^-$	$1.4\times10^{10}\ M^{-1}\cdot s^{-1}$
$Cl_2^- + O_2^- \rightarrow 2Cl^- + O_2$	$1\times10^9\ M^{-1}\cdot s^{-1}$
$Cl_2^- + H_2O_2 \rightarrow 2Cl^- + H^+ + HO_2^{\cdot}$	$1.4\times10^5\ M^{-1}\cdot s^{-1}$

the highly acidic solution, this reaction should not propagate the chain. It should also be noted that the reaction of Cl^- with O_3 is negligible due to its very low rate constant of $3\times10^{-3}\ M^{-1}\cdot s^{-1}$ (Hoigne et al., 1985). Hence, according to the existing literature, HCl is not expected to promote the decomposition of ozone. To confirm this hypothesis, the experiments were conducted at various concentrations of HCl in the range of 0.02–0.2 N.

Before the photolysis experiments were started, ozone gas was sparged into the HCl solution until the ozone concentration in the solution was stabilized. Ozone dosage was kept at 45 mg per liter of gas for all the experiments. The ozone concentrations reached under these conditions were observed to vary inversely with the strength of the HCl solution. This is probably due to the inverse dependence of ozone solubility on the ionic strength of the solution (Gurol and Singer, 1982). After the ozone gas was turned off, the solutions were exposed to the UV radiation.

The aqueous ozone concentration measured as a function of time at various HCl concentrations and a UV light intensity of 4.4×10^{-6} einstein/L-s is shown in Figure 3. These experimental results support the contention that ozone decomposition reaction is zero order with respect to ozone concentration when the secondary reactions are quenched effectively (Eq. 26). The zero-order rate constant determined from the slopes of the straight lines for different HCl concentrations is equal to $(2.18\pm0.08)\times10^{-6}\ M\cdot s^{-1}$. Furthermore, there is no apparent dependence of the rate constant on the solution strength, confirming that reactions of Cl^- do not promote ozone decomposition.

In Figure 4, the ozone concentration is shown as a function of time for various light intensities in 0.1 N of HCl solution.

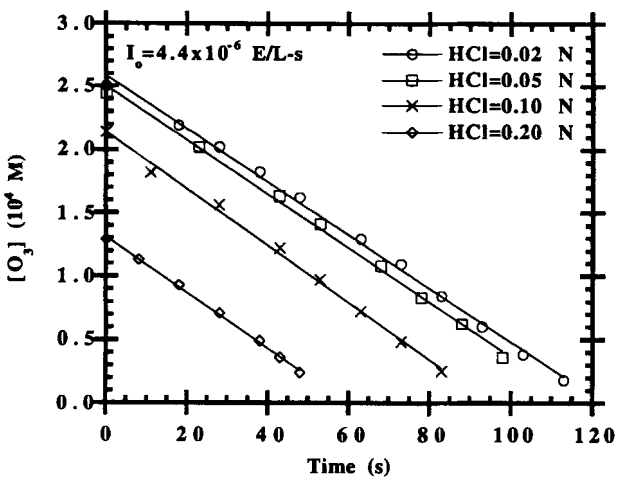

Figure 3. Photolysis of ozone in HCl solutions.

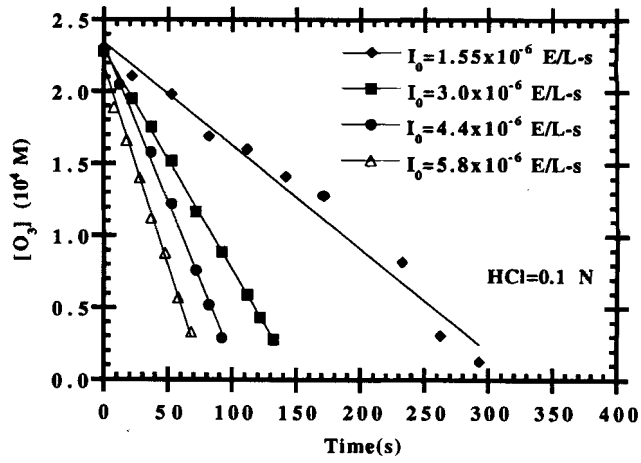

Figure 4. Photolysis of ozone at various light intensities.

The zero-order rate constant ($k_o = \phi_p I_o$) was calculated from the slopes of the straight lines of the ozone profiles, and replotted as a function of the corresponding I_o in Figure 5. The slope of the straight line in this figure yields ϕ_p as 0.48 $\pm$0.06. Taube (1956) reported the quantum yield of ozone disappearance in acetic acid solution at a wavelength of 254 nm as 0.62. The higher quantum yield reported by Taube could be because of the nonspecific iodometric method used for ozone measurement. Hydrogen peroxide and organic peroxides interfere with the iodometric measurement of ozone. Furthermore, acetic acid may not provide enough radical scavenging capacity, and may also promote ozone decomposition.

Ozone photolysis in gas phase has been investigated in the UV wavelength range of 248–266 nm by several investigators (Biedenkapp and Bair, 1970; Jones and Wayne, 1970; Philen et al., 1977). It was suggested that the photolysis of ozone in gas produces excited oxygen atom $O(^1D)$ and ground state oxygen atom $O(^3P_j)$, which propagate the chain reaction leading to further ozone decomposition. Based on the measurements of $O(^1D)$ and $O(^3P_j)$, the primary quantum yield for gaseous ozone decomposition was reported to be about

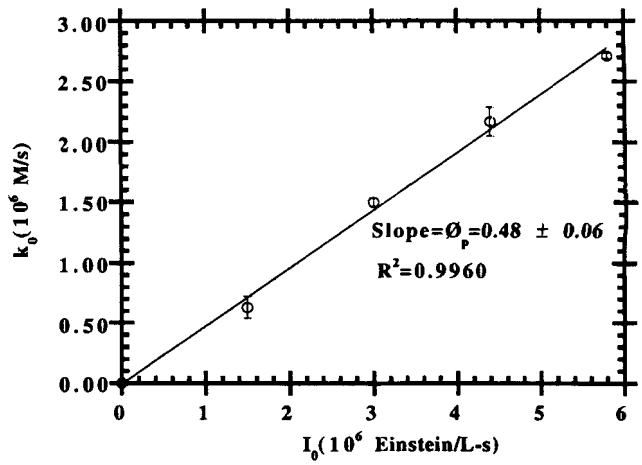

Figure 5. Ozone photolysis rate constant vs. UV light intensity.

1.0. Hence, it can be concluded that the primary quantum yield of ozone photolysis in the UV wavelength of about 254 nm in aqueous solution is about half of the yield in the gas phase.

Effective Optical Path Length in the Experimental Reactor for Hydrogen Peroxide

The light path for hydrogen peroxide in the experimental reactor was determined by measuring the photolysis rate of H_2O_2 at a low concentration (2.3×10^{-4} M) to make sure that Eqs. 28 and 29 would be applicable. Allyl alcohol at 0.1 M was added to the solution as a scavenger for $OH^{\cdot}$ radicals in order to quench the secondary reactions (Volman and Chen, 1959). The solution pH was then adjusted to 7. Under these conditions, the decomposition of hydrogen peroxide can be described by Eq. 29, which upon integration for a batch reactor yields:

$$\ln([H_2O_2]/H_2O_2)_o = -2.3\Phi'_p a' b_{\text{eff}} I_o t = -k_1 t \quad (31)$$

This expression indicates that the first-order rate constant (k_1) to be obtained for decomposition of H_2O_2 will be a function of Φ'_p, I_o, a', and b_{eff}. In Figure 6, the results of the experiments with H_2O_2 are presented according to Eq. 31. The decomposition of H_2O_2 follows a first-order reaction with respect to H_2O_2 concentration, as expected. The first-order reaction rate constant (k_1) calculated for each I_o was replotted as a function of the corresponding I_o in Figure 7. For $\Phi'_p = 0.5$ and $a' = 19.6$ $M^{-1}\cdot cm^{-1}$, b_{eff} was estimated from the slope of the straight line in Figure 7 as 10.3 ± 1.9 cm. This is a reasonable value for b_{eff}, considering that the reactor used in this study has an inner diameter of 13 cm.

Method of Solution of the Model Equations

The average rates of change of ozone and hydrogen peroxide concentrations in the O_3/UV process can now be described by Eqs. 22–29. The solution to these equations, which include two nonlinear ordinary differential equations, is not accessible by analytical methods. In this study, a computer

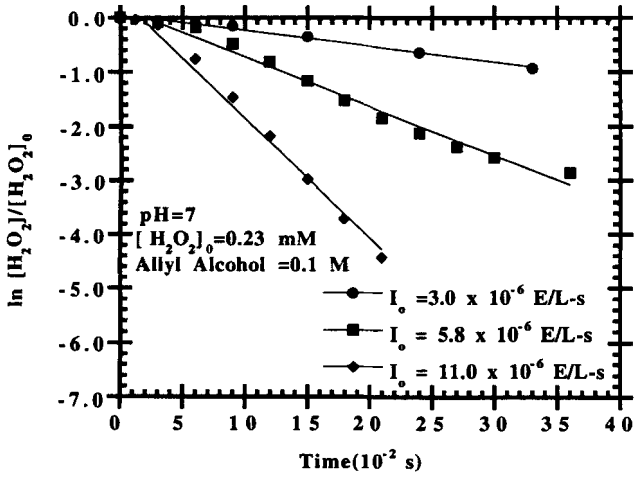

Figure 6. Photolysis of hydrogen peroxide by UV radiation.

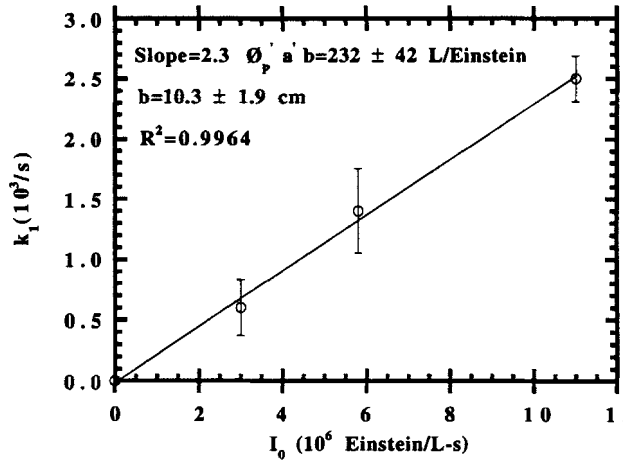

Figure 7. Hydrogen peroxide photolysis rate constant vs. UV light intensity.

program was designed on a spreadsheet (Excel 4.0) by using the fourth-order Runga-Kutta algorithm to solve the equations numerically (Gerald and Wheatley, 1983). The two differential equations (Eqs. 22 and 23) were first reduced to a function of only the concentration of the two stable molecules, ozone, and hydrogen peroxide. This was accomplished by assuming steady-state conditions for all the radical species and instantaneous equilibrium for all the acid/base conjugates. The initial ozone concentration, the light intensity, the water characteristics in terms of the pH, the total inorganic carbon concentrations, and the values of the rate constants were provided as inputs into the computer program. The time step for the integration process was set at 0.5 s, which was sufficient to provide negligible round-off error at each time step. The program was run to predict the concentrations of ozone and hydrogen peroxide as a function of time within the desired time interval.

It was found that the contribution of the radical–radical termination reactions, presented by Eqs. 11–13, to the overall reaction mechanism was negligible due to very low radical concentrations. The contribution of self-decomposition of ozone described by Eq. 14 was also negligible due to very small rate constant. The sensitivity of the model was also tested for k_i, which is the rate constant of the reactions of $HCO_3^{\cdot}$ and $CO_3^{\cdot-}$ by any reactant other than H_2O_2/HO_2^-. Since in our test solutions, carbonate ions were the only such reactants, and there is no information in the literature regarding the rate of these reactions, it was assumed that $HCO_3^{\cdot}$ and $CO_3^{\cdot-}$ react with carbonate ions with an unknown rate constant of k_i. The sensitivity of the model to k_i was then tested by solving the model equations for k_i values in the range of 10^5 to 10^9 M^{-1} s^{-1} for various concentrations of total inorganic carbon, C_T, in the range of 0.8–10 mM. It should be noted that the typical rate constants for the reaction of $CO_3^{\cdot-}$ with inorganic species are in the range of 10^5–10^9 M^{-1} s^{-1} (Behar et al., 1970). The results of this analysis showed that ozone and hydrogen peroxide concentrations were not sensitive to the value of k_i in the range of interest. On the other hand, the model equation predicted that $HCO_3^{\cdot}$ and $CO_3^{\cdot-}$ will primarily be trapped by the carbonate ions, and the amount of $HCO_3^{\cdot}$ and $CO_3^{\cdot-}$ that is ex-

pected to react with H_2O_2/HO_2^- would be very small in the presence of inorganic carbon even at a concentration of 0.8 mM.

Under these conditions, the average decomposition rate of ozone is reduced to a mixed order with respect to ozone concentration, with apparent rate constants that are functions of measurable parameters, as presented below:

$$-d[O_3]/dt = C + C^*[O_3] + C^{**}[O_3]^2 \quad (32)$$

where

$$C = \phi_p I_o \quad (33)$$

$$C^* = 2k_4^*[H_2O_2] + \frac{4.6k_{10}a'b_{\text{eff}}\phi_p' I_o[H_2O_2]}{k_{15}^*[HCO_3^-]} \quad (34)$$

$$C^{**} = \frac{4k_{10}k_4^*[H_2O_2]}{k_{15}^*[HCO_3^-]} \quad (35)$$

and

$$k_4^* = (k_4 K_{a,3})/[H^+] \quad (36)$$

$$k_{15}^* = (k_{15}[H^+] + k_{16}K_{a,3})/[H^+] \quad (37)$$

Here, C is an ozone-independent coefficient, and C^* and C^{**} are the coefficients of the terms that are first- and second-order with respect to ozone, respectively. The zero-order term describes the primary photolysis of ozone. In C^* the first term describes the reaction of ozone with HO_2^-, and the second term describes the reaction of ozone with $OH^\cdot$ radical, which is produced directly from the photolysis of hydrogen peroxide. The rate of the latter reaction decreases in the presence of carbonate ions due to radical scavenging. The second-order term describes the reaction of ozone by $OH^\cdot$ radical, which is produced as a result of the chain reactions initiated by the reaction of ozone with HO_2^- species. This term also includes the effect of carbonate scavenging. The amount of contribution of each term to the rate of ozone decomposition determines the overall order of the reaction and the magnitude of the observed reaction rate at a given condition.

The concentration of hydrogen peroxide can be presented as

$$d[H_2O_2]/dt = D - D^*[H_2O_2] - D^{**}[H_2O_2]^2 \quad (38)$$

where

$$D = C = \phi_p I_o \quad (39)$$

$$D = \phi_p I_o \quad (40)$$

$$D^* = k_4^*[O_3] + 2.3a'b_{\text{eff}}\phi_p' I_o \quad (41)$$

$$D^{**} = \frac{4.6a'b_{\text{eff}}\phi_p' I_o k_5^* + 2k_4^* k_8^*[O_3]}{k_{15}^*[HCO_3]} \quad (42)$$

and

$$k_8^* = (k_8[H^+] + k_9 K_{a,3})/[H^+] \quad (43)$$

Table 3. Values of Parameters used in Experiments and the Model Simulation

Parameter	Base Value	Values Tested
UV intensity (einstein/L·s)	1.5×10^{-6}	1.5×10^{-6}–11.0×10^{-6}
Initial ozone concentration (mM)	0.25	0.25–0.0625
pH	7	6–9
C_T (mM)	0.8	0.8–10

The sensitivity of the model equations to ϕ_p was tested for the ϕ_p values of 0.48 and 0.62, the value reported by Taube (1957). The difference in the predicted ozone concentrations for these two values was about 7%, which is in the range of the experimental measurement error. For the rest of the modeling efforts, the ϕ_p of 0.48 was substituted in the model equations. The program was run to predict the profiles of ozone and hydrogen peroxide for the selected base and the range of the parameters listed in Table 3.

Results and Discussion

Effect of UV light intensity

The measured and predicted ozone concentration profiles are presented on normalized basis in Figure 8 as a function of time at various light intensities. The initial ozone concentration is 0.25 mM (12 mg/L) for all the experiments. The results show that increasing the light intensity increases the rate of ozone decomposition, and the prediction of the model coincides very well with the experimental data for the base conditions listed in Table 3. According to the model equations (Eqs. 32–43), the primary rate of ozone photolysis increases directly with light intensity, and furthermore the rate of the secondary reactions accelerate due to faster formation of hydrogen peroxide as an intermediate. The calculations revealed that all three terms in Eq. 32 contributed about equally to the overall decay rate of ozone. Hence, it can be concluded that the first-order decay with respect to ozone concentration as reported by Ikemizu (1987) is only an empirical force fitting of this complex kinetic expression to the experimental data.

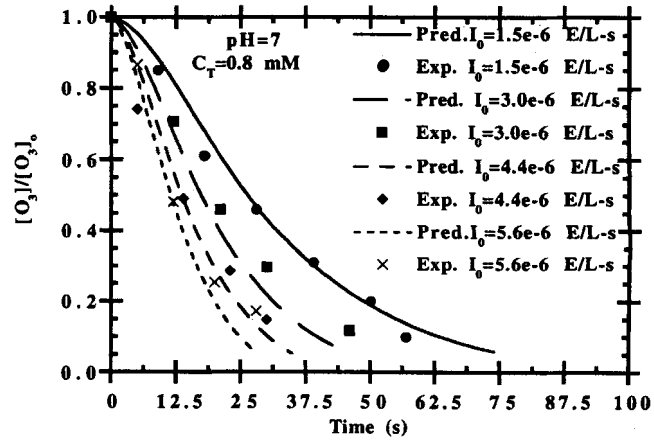

Figure 8. Comparison of predicted and measured ozone profiles for various UV light intensities.

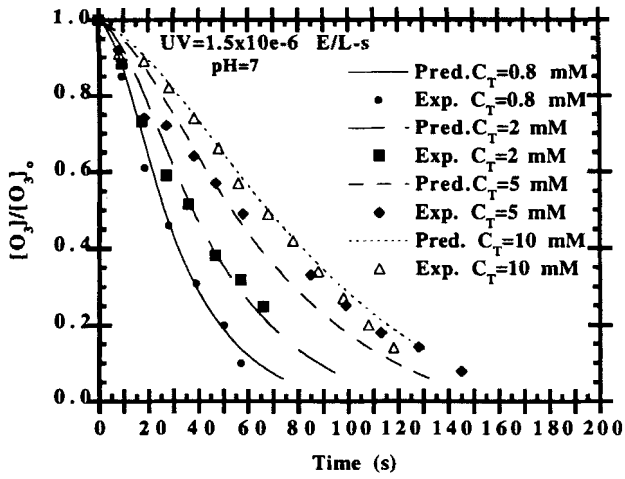

Figure 9. Comparison of predicted and measured ozone profiles for various C_T values.

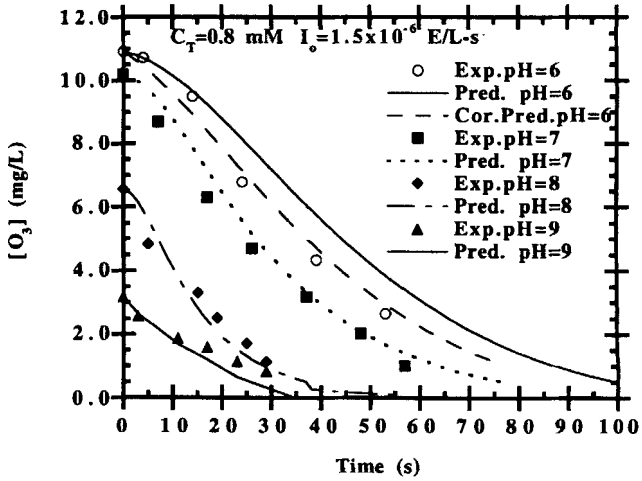

Figure 10. Comparison of predicted and measured ozone profiles at various pH.

Effect of C_T

The experimentally observed and predicted ozone decomposition profiles are presented in Figure 9 for various C_T values. The initial ozone concentration is kept at 0.25 mM for all the experiments. The results clearly show that increasing the concentration of the carbonate/bicarbonate at a constant pH causes a retardation on the decomposition rate of ozone. This supports the contention that the secondary reaction of ozone with hydroxyl radical is successfully suppressed in the presence of radical scavenging carbonate ions. The same carbonate effect is also observed on the rate of self-decomposition of ozone that is initiated by hydroxide ion (Hoigne, 1976). The photokinetic model predicted the experimental data presented in Figure 9 very well, further confirming that the assumptions made in reducing the model to Eqs. 32–43 were justified under the experimental conditions of this study.

Effect of pH

The experimental data and the model predictions on the decomposition of ozone at various pH values are presented in Figure 10. Here, ozone decomposition profiles were plotted for the absolute concentrations of ozone rather than the normalized concentrations. This was because of obtaining different initial ozone concentrations at different pH values prior to exposure to UV radiation due to self-decomposition of ozone (Eq. 14). According to the experimental data presented in this figure, the rate of ozone photolysis was not affected by the pH significantly. A similar observation was made earlier by Morooka et al. (1988), who reported that ozone decomposition rate was proportional to hydroxide ion concentration with only an order of 0.07.

According to the reaction mechanism presented earlier, the pH could affect the rate of ozone photolysis in two ways. Increasing the pH increases the dissociation of H_2O_2 to HO_2^-, and as a result accelerates the reaction rate of ozone with HO_2^-. Secondly, an increase in the pH is expected to reduce the concentration of $OH^\cdot$ by shifting the $HCO_3^-/CO_3^=$ equilibrium to $CO_3^=$, which is a more effective $OH^\cdot$ scavenger than HCO_3^- (Table 4); this should reduce the rate of the secondary reaction of ozone with $OH^\cdot$. Therefore, these two opposing reaction pathways may result in a net no-pH effect.

The ozone profiles predicted by the kinetic model fit the experimental observations reasonably well at pH 7 and 8. The model predicted a slower rate at pH 6 (see the solid line for pH 6 in Figure 10). In addition to the reaction pathways presented by Reactions 1–7, it was reported (Yao et al., 1992) that less than 5% of the $OH^\cdot$ radical could be produced directly from the photolysis of ozone by the following pathway:

$$O_3 + H_2O \xrightarrow{h\nu} 2OH^\cdot + O_2 \qquad (44)$$

Hence, the sensitivity of the model to this pathway was investigated by including this reaction step in the model. In the absence of any other information, varying percentages were assigned for this pathway of direct photolysis of ozone to $OH^\cdot$ (Eq. 44) vs. the pathway that leads to hydrogen peroxide formation from photolysis of ozone (Eq. 1). The model was found sensitive to the direct pathway at pH 6 but not at pH 7–9. At pH 6, a good agreement with the experimental observations was obtained when it was assumed that 2% of ozone decomposes according to Eq. 44 (see the dashed line in Figure 10 for pH 6).

At pH 9 the model predicted slightly faster decomposition rate, probably because the ozone measurement technique is relatively insensitive at lower ozone concentrations. In fact, when the experiments were repeated at pH 9 for a C_T value of 5 mM where an initial ozone concentration as high as 7.8 mg/L was produced, the fit of the model predictions to the experimental data has much improved.

Table 4. Relative Effect of pH on Scavenging of $OH^\cdot$ by $HCO_3^-/CO_3^=$ Ions for C_T = 0.8 mM

pH	Relative Effectiveness of $OH^\cdot$ Scavenging
6.0	1.0
7.0	2.36
8.0	3.14
9.0	6.82

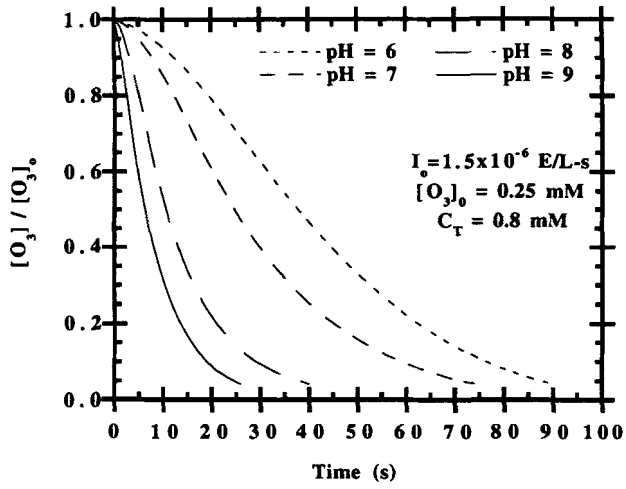

Figure 11. Predicted ozone profiles at various pH for equal initial ozone concentration.

Since the rate of ozone photolysis is a function of ozone concentration, and lower initial ozone levels can be maintained at higher pH values, an attempt was made to uncouple the pH effect from the effect of ozone concentration by running the program of the kinetic model for the same initial ozone concentrations at various pH values. The predicted ozone profiles presented in Figure 11 indicate that the rate of ozone photolysis should increase significantly with increasing pH. Hence, the experimental observation of no significant pH effect was probably an artifact of varying initial ozone concentration.

Summary and Conclusions

The kinetics of ozone photolysis under UV exposure were investigated by laboratory experiments as well as a kinetic model developed based on known possible reaction pathways. The primary quantum yield of ozone photolysis was determined as 0.48 ± 0.06 at 254 nm wavelength and 20°C. This information was then used to describe the effect of pH and inorganic carbon (C_T) in water on the rate and mechanism of ozone photolysis. It was demonstrated that the rate of ozone photolysis increased with increasing incident light intensity, ozone concentration, and pH, and decreased with increasing C_T. A kinetic model of the process, which is a complex function of the primary quantum yield, the incident UV light intensity, initial ozone concentration, the effective optical path length of the reactor system, and water characteristics that include the pH and the total inorganic carbon content, was developed and tested. The model was able to predict the experimentally measured rate of ozone photolysis quite well for various combinations of UV light intensities, initial ozone concentrations, and water characteristics.

In the O_3/UV process, organic and inorganic contaminants in water and wastewaters are primarily oxidized by the hydroxyl radical that is generated from ozone photolysis. This research provides kinetic information on the hydroxyl radical formation and consumption as well as ozone photolysis under various operational and water quality conditions. Therefore, this information on hydroxyl radical is directly related to the oxidation rate and mechanisms of the contaminants. The parameters identified here as having promotional or hindering effect on the rate of ozone photolysis are expected to affect the oxidation rates of the contaminants the same way. For sample, the oxidation rates are expected to increase with increasing incident light intensity, ozone concentration, and pH, and decrease with increasing C_T of the water. However, certain organic compounds (chromophores) can directly photolyze under UV exposure in addition to being oxidized with hydroxyl radical. Furthermore, the pH of water also determines the dominant form of the species for ionizable contaminants, and the reactivity of the hydroxyl radical with each species should be taken into consideration as well.

The kinetic ozone photolysis model developed in this study can readily be incorporated into a comprehensive model describing the oxidation of contaminant(s) in the O_3/UV process. Such a model should also include the terms for the rate of ozone mass transfer from gas into liquid, the rate of oxidation of the contaminant(s), and the reaction intermediates by the hydroxyl radical and the rate of direct photolysis of the contaminant(s) and the intermediates. This is the subject of an article currently under preparation based on a PhD dissertation (Akata, 1994).

Acknowledgments

This research was financially supported by the National Science Foundation through the Environmental Engineering Program (BCS-9020028).

Literature Cited

Akata, A., and M. D. Gurol, "Photocatalytic Oxidation Processes in the Presence of Polymers," *Ozone Sci. Eng.*, **14**, 367 (1992).

Arai, H., M. Arai, and A. Sakumoto, "Exhaustive Degradation of Humic Acid in Water by Simultaneous Application of Radiation and Ozone," *Water Res.*, **20**(7), 885 (1986).

Bader, H., and J. Hoigne, "Determination of Ozone in Water by the Indigo Method," *Water Res.*, **15**, 449 (1981).

Bahnemann, D., and E. J. Hart, "Rate Constants of the Reaction of the Hydrated Electron and Hydroxyl Radical with Ozone in Aqueous Solution," *J. Phys. Chem.*, **88**, 5999 (1984).

Barker, R., and F. M. Taylor, "Oxidation of 2-Propanol in Dilute Aqueous Solution by UV/Ozone," *Proc. Int. Conf. on the Role of Ozone in Water and Wastewater Treatment*, London (1985).

Baxendale, J. H., and J. A. Wilson, "The Photolysis of Hydrogen Peroxide at High Light Intensities," *Trans. Faraday Soc.*, **53**, 344 (1956).

Behar, D., G. Czapski, and I. Duchovny, "Carbonate Radical in Flash Photolysis and Pulse Radiolysis of Aqueous Carbonate Solutions," *J. Phys. Chem.*, **74**, 2206 (1970).

Biedenkapp, D., and E. J. Bair, "Ozone Ultraviolet Photolysis. I. The Effect of Molecular Oxygen," *J. Chem. Phys.*, **52**(12), 6119 (1970).

Bielski, B. H. J., and A. O. Allen, "Mechanism of the Disproportionation of Superoxide Radicals," *J. Phys. Chem.*, **81**, 1048 (1977).

Buhler, R. E., J. Staehelin, and J. Hoigne, "Ozone Decomposition in Water Studied by Pulse Radiolysis. 1. HO_2/O_2^- and HO_3/O_3^- as Intermediates," *J. Phys. Chem.*, **88**, 2560 (1984).

Chameides, W. L., and A. W. Stelson, "Aqueous-Phase Chemical Processes in Deliquescent Sea-Salt Aerosols: A Mechanism That Couples the Atmospheric Cycles of S and Sea Salt," *J. Geophys. Res.*, **97**, 20, 565 (1992).

Christensen, H. S., K. Sehested, and H. Corftizan, "Reactions of Hydroxyl Radicals with Hydrogen Peroxide at Ambient and Elevated Temperatures," *J. Phys. Chem.*, **86**, 1588 (1982).

Eriksen, T. E., J. Lind, and G. Merenyi, "On the Acid-Base Equilibrium of the Carbonate Radical," *Radiat. Phys. Chem.*, **26**, 197 (1985).

Farhataziz, and A. B. Ross, "Selected Specific Rates of Reactions of

Transients for Water in Aqueous Solution: III. Hydroxyl Radical and Perhydoxyl Radical and Their Radical Ions," *Nat. Std. Ref. Data Ser.*, U. S. Nat. Bur. of Std., p. 59 (1977).

Garrison, R. L., C. E. Mauk, and H. W. Prengle, Jr., "Advanced Ozone Oxidation System for Complexed Cyanides," *Proc. Int. Symp. on Ozone for Water and Wastewater Treatment*, R. G. Rice and M. E. Browning, eds., International Ozone Institute, Syracuse, NY, p. 551 (1975).

Gerald, C. S., and P. O. Wheatley, *Applied Numerical Analysis*, Addison-Wesley, Reading, MA, p. 332 (1983).

Glaze, W. H., G. R. Peyton, S. Lin, F. Y. Huang, and J. L. Burleson, "Destruction of Pollutants in Water with Ozone in Combination with Ultraviolet Radiation. 2. Natural Trihalomethane Precursors," *Environ. Sci. Technol.*, **16**, 454 (1983).

Gurol, M. D., and P. C. Singer, "Kinetics of Ozone Decomposition: A Dynamic Approach," *Environ. Sci. Technol.*, **16**, 377 (1982).

Gurol, M. D., and R. Vatistas, "Oxidation of Phenolic Compounds by Ozone and Ozone + UV Radiation: A Comparative Study," *Wat. Res.*, **21**, 895 (1987).

Hatchard, C. G., and C. A. Parker, "A New Sensitive Chemical Actinometer: II. Potassium Ferrioxalate as a Standard Chemical Actinometer," *Proc. R. Soc. London Ser. A.*, **235**, 518 (1956).

Hoigne, J., H. Bader, W. R. Haag, and J. Staehelin, "Rate Constants of Reactions of Ozone with Organic and Inorganic Compounds in Water, III," *Water Res.*, **19**, 993 (1985).

Hunt, J. P., and H. Taube, "The Photochemical Decomposition of Hydrogen Peroxide. Quantum Yields, Tracer and Fractionation Effects," *J. Amer. Chem. Soc.*, **74**, 5999 (1952).

Ikemizu, I., M. Orita, M. Sagiike, S. Morooka, and Y. Kato, "Ozonation of Organic Refractory Compounds in Water in Combination with UV Radiation," *J. Chem. Eng. Japan*, **20**, 369 (1987).

Jayson, G. G., B. J. Parsons, and A. J. Swallow, "Oxidation of Ferrous Ions by Perhydroxyl Radical," *J. Chem. Soc. Faraday Trans. I*, **69**, 236 (1972).

Johnson, J. L., and M. D. Gurol, Removal of Trace Organic Chemicals by Ozone, UV and Ozone + UV," *Proc. of Env. Eng.*, CSCE-ASCE, Vancouver, Canada, p. 447 (1988).

Jones, I. T. N., and R. P. Wayne, "The Photolysis of Ozone by Ultraviolet Radiation IV. Effect of Photolysis Wavelength on Primary Step," *Proc. R. Soc. London Ser. A.*, **319**, 273 (1970).

Kearney, P. C., M. T. Muldoon, and C. J. Somich, "UV-Ozonation of Eleven Major Pesticides as a Waste Disposal Pretreatment," *Chemosphere*, **16**(10–12), 2321 (1987).

Khan, S. R., C. R. Huang, and J. W. Bozzelli, "Oxidation of 2-Chlorophenol using Ozone and Ultraviolet Radiation," *Environ. Prog.*, **4**(4), 229 (1985).

Kuo, P. P., E. S. K. Chian, and B. J. Chang, "Identification of End Products Resulting from Ozonation and Chlorination of Organic Compounds Commonly Found in Water," *Environ. Sci. Technol.*, **11**(13), 1177 (1977).

Larson, T. E., and A. M. Buswell, "Calcium Carbonate Saturation Index and Alkalinity Interpretations," *J. Amer. Water Works Assoc.*, **34**, 1664 (1942).

Liao, C. H., and M. D. Gurol, "Chemical Oxidation by Photolytic Decomposition of Hydrogen Peroxide," *Environ. Sci. Technol.*, **29**, 3007 (1995).

Morooka, S., K. Kusakabe, J. Hayashi, K. Isomura, and K. Ikemuzu, "Decomposition and Utilization of Ozone in Water Treatment Reactor with Ultraviolet Radiation," *Ind. Eng. Chem. Res.*, **27**, 2372 (1988).

Parker, C. A., "A New Sensitive Chemical Actinometer: I. Some Trials with Potassium Ferrioxalate," *Proc. R. Soc. London Ser. A.*, **220**, 104 (1953).

Peyton, G. R., F. Y. Huang, J. L. Burleson, and W. H. Glaze, "Destruction of Pollutants in Water with Ozone in Combination with Ultraviolet Radiation. 1. General Principles and Oxidation of Tetrachloroethylene," *Environ. Sci. Technol.*, **16**, 448 (1982).

Peyton, G. R., and W. H. Glaze, "Destruction of Pollutants in Water with Ozone in Combination with Ultraviolet Radiation. 3. Photolysis of Aqueous Ozone," *Environ. Sci. Technol.*, **22**, 761 (1988).

Philen, D. L., R. T. Watson, and D. D. Davis, "A Quantum Yield of Determination of O(1D) Production from Ozone via Flash Photolysis," *J. Chem. Phys.*, **67**(7), 3116 (1977).

Prengle, H. W., "Experimental Rate Constants and Reactor Considerations for the Destruction of Micropollutants and Trihalomethane Precursors by Ozone with Ultraviolet Radiation," *Environ. Sci. Technol.*, **17**(12), 743 (1983).

Rabani, J., and S. O. Nielsen, "Absorption Spectrum and Decay Kinetics of O_2^- and HO_2 in Aqueous Solutions by Pulse Radiolysis," *J. Phys. Chem.*, **73**, 3736 (1969).

Sauer, M., Jr., W. G. Brown, and E. J. Hart, *J. Phys. Chem.*, **88**, 1398 (1984).

Staehelin, J., and J. Hoigne, "Decomposition of Ozone in Water: Rate of Initiation by Hydroxide Ions and Hydrogen Peroxide," *Env. Sci. Technol.*, **16**, 672 (1982).

Standard Method for the Examination of Water and Wastewater, APHA, AWWA, WPCF, Washington, DC (1985).

Taube, H., "Photochemical Reactions of Ozone in Solution," *Trans. Faraday Soc.*, **53**, 565 (1957).

U.S. EPA—RREL, *Site Program Demonstration of the Ultrox International Ultraviolet Radiation/Oxidation Technology*, Technol. Eval. Rep., EPA/540/5-89/012 (1990).

Volman, D. H., and J. C. Chen, "The Photochemical Decomposition of Hydrogen Peroxide in Aqueous Solutions of Allyl Alcohol at 2537 Ao," *J. Amer. Chem. Soc.*, **81**, 4141 (1959).

Weeks, J. L., and J. Rabani, "The Pulse Radiolysis of Deaerated Aqueous Carbonate Solutions. I. Transient Optical Spectrum and Mechanism. II. pK for OH Radicals," *J. Phys. Chem.*, **70**(7), 2100 (1966).

Yao, C. C. D., W. R. Haag, and T. Mill, "Kinetic Features of Advanced Oxidation Processes for Treating Aqueous Chemical Mixtures," *Proc. Int. Symp. Chemical Oxidation Technology for the Nineties*, Nashville, TN (1992).

Manuscript received Jan. 19, 1996, and revision received Apr. 15, 1996.